Design and DEM simulation analysis of shaped groove eyelet wheel rapeseed precision seed dispenser

Gang Rao[1,2], Wuyun Zhao[1], Linrong Shi[1*], Xin Chen[2], Bugong Sun[1], Zun Wang[1], Hui Li[1]
(1. *School of Mechanical and Electrical Engineering, Gansu Agricultural University, Lanzhou 730070, China*;
2. *School of Automation, China University of Geosciences, Wuhan 430074, China*)

Abstract: To address the challenges of low precision and suboptimal seeding efficiency in existing rapeseed seed metering wheels equipped with shaped grooves, the traditional rectangular grooves were redesigned into trapezoidal forms to enhance overall seeding performance. Building upon this modification, a precision metering wheel featuring trapezoidal-shaped grooves capable of dispensing (3±1) seeds per hole was developed, and its fundamental structural parameters were established. Theoretical analysis combined with experimental validation identified four key factors influencing seed filling performance: the inclination angle of the seed guide shaped groove, the rotational speed of the metering wheel, the width of the trapezoidal groove, and the non-standard opening width. A response surface methodology was employed to examine the effects of these factors on the qualification rate, reseeding rate, and missed seeding rate. Results indicated that the qualified seeding rate was 94.17%, the reseeding rate was 3.92%, and the missed seeding rate was 1.91% under optimal parameters. Field tests confirmed that the device met the agronomic requirements for rapeseed sowing. This study serves as a reference for the design of precision sowing devices for rapeseed.

Keywords: rapeseed, shaped groove eyelet wheel, response surface methodology, precision sowing
DOI: 10.25165/j.ijabe.20251805.9552

Citation: Rao G, Zhao W Y, Shi L R, Chen X, Sun B G, Wang Z, et al. Design and DEM simulation analysis of shaped groove eyelet wheel rapeseed precision seed dispenser. Int J Agric & Biol Eng, 2025; 18(5): 102–116.

1 Introduction

Rapeseed is one of the principal oilseed crops extensively cultivated in China[1]. As the area dedicated to rapeseed cultivation expands, challenges in the planting process have become increasingly pronounced, particularly concerning mechanization levels and sowing accuracy[2]. Despite advances in science and technology that have yielded sophisticated sowing machines, the majority remain unsuitable for rapeseed planting in the Gansu region of northwest China, thereby constraining the economic development of the rapeseed industry in this area[3]. Consequently, there is an urgent need to tackle issues such as low-precision seeding in rapeseed cultivation within the Gansu region to foster sustainable economic development[4].

Seed displacers play a vital role in achieving precision sowing, with the most commonly used types for rapeseed primarily comprising mechanical and pneumatic systems[5]. The development of seed displacers in Europe and the United States began earlier, resulting in a strong theoretical foundation and considerable manufacturing expertise. Research by Arzu Yazgi et al.[6] employed response surface methodology to explore the factors affecting the uniformity of grain spacing for small seeds with high sphericity in pneumatic suction seeders. Their findings indicate that both the diameter of the suction holes and the degree of vacuum significantly impact sowing accuracy. Nikola et al.[7] conducted a comparative analysis of mechanical and air-assisted seeders, examining various forward speeds and carriers to identify the optimal seeding implement and speed needed to meet precision sowing requirements in different environments. The SIGMA 5 air-assisted seeder, introduced by SFOGGIA in Italy, combines air-assisted and mechanical features. Its innovative design, featuring a curved four-toothed seed picker, a seed rotating needle, and a seed-separating needle structure, effectively addresses issues of seed leakage and reseeding. This design significantly reduces seed breakage rates during the intake and ejection processes, ensuring precise seed placement and maintaining consistent plant spacing. Europe and the United States have advanced sophisticated seed drill technology primarily designed for expansive, flat fields. Nevertheless, the substantial costs and intricate operational demands present considerable obstacles to adaptation to China's varied terrain. As a result, Chinese researchers have conducted comprehensive investigations to develop seed drills customized to local conditions. Shi et al.[8] engineered a mechanical-pneumatic combination seed dispenser, based on the principles of overpressure airflow and guide grooves, which streamlines the complex morphological structure of air-suction seed dispensers while significantly improving seed-filling efficiency. Wu et al.[9] created a hybrid positive and negative air pressure air-suction seeder suitable for small seed crops such as rapeseed, examining the effects of different hole designs on airflow uniformity. Their results revealed that a cylindrical structure provides enhanced stability, and increasing the depth of the air chamber in the seed filling region further maximizes filling efficiency. As the predominant seed discharger in the market, air

Received date: 2024-11-17 **Accepted date:** 2025-07-10
Biographies: **Gang Rao**, PhD candidate, research interest: agricultural engineering, Email: 625678563@qq.com; **Wuyun Zhao**, Professor, research interest: crop production equipment engineering in northern arid areas, Email: zhaowy@gsau.eu.cn; **Xin Chen**, Professor, research interest: control science and engineering, Email: chenxin@cug.edu.cn; **Bugong Sun**, Professor, research interest: full mechanization of dryland agriculture, Email: sunbg@gsau.edu.cn; **Zun Wang**, MS, research interest: agricultural machinery, Email: 2323908271@qq.com; **Hui Li**, MS, research interest: precision seeding equipment, Email: 2133996862@qq.com.
***Corresponding author: Linrong Shi**, Associate Professor, research interest: agricultural mechanization engineering. Gansu Agricultural University, Lanzhou, Gansu Province 730070, China. Tel: +86-18152092689, Email: shilr@gsau.edu.cn.

suction seed dischargers are characterized by high productivity, efficient operation, low seed damage rates, and excellent adaptability to various seed types. However, the complexity of their structure, coupled with high processing costs and the instability of wind forces, results in significant errors in operational performance[10,11]. Although eye socket wheel mechanical seeders exhibit structural simplicity and operational stability, their seeding efficiency is significantly constrained by gravity-dependent filling mechanisms. Small-grain rapeseed, characterized by low mass and poor flowability, is susceptible to airflow interference during the filling process, resulting in inconsistent seed distribution. Furthermore, the geometric rigidity of seeding apertures—manifested as fixed thickness or non-tapered designs—fails to accommodate variations in rapeseed triaxial dimensions. This limitation exacerbates seed disturbance and compromises seeding precision[12]. Although their adaptability to different seeds is limited, these devices offer a simple, cost-effective, and farmer-friendly structure, alongside stable performance. Liu et al.[13] optimized and enhanced the spatial characteristics of seeds encapsulated within the holes by analyzing the structural design of the rapeseed nest-eye wheel seed discharger. Their objective was to mitigate seed population disturbance and improve the filling performance of the discharger. In parallel, Lai et al.[14] employed a methodology whereby increasing population disturbance was found to reduce local friction among seeds, leading to the design of a shaped nest-eye wheel seed discharger featuring a convex hole structure. This innovation effectively addressed high damage rates associated with ginseng seeds, as well as mobility and leakage issues during the filling process, thereby significantly enhancing filling efficiency. The shaped hole constitutes a critical element of the eyelet wheel seed dispenser, with its structural composition and shape distribution directly influencing seeding accuracy[15]. Mechanical seeders are widely adopted owing to their structural simplicity and cost-effectiveness. However, their fixed-aperture configurations present notable limitations. Peng et al.[16] demonstrated through bench experiments that seeds with irregular morphologies—such as industrial hemp (diameter 0.8-1.2 mm) and rapeseed (length 12-15 mm)—are particularly susceptible to overseeding or missed seeding due to dimensional inconsistencies. During high-speed operations, shaped groove-type seeders exhibit seed filling qualification rates of merely 70%-80%, primarily due to vibrational disturbances. Moreover, fluctuations in ambient humidity can exacerbate seed adhesion and lead to groove blockages. Currently, fluted wheel seed expellers in the Chinese market encounter challenges related to a lack of structural diversity, which hampers their ability to meet the agronomic requirements of rapeseed cultivation in the northwestern arid zone. Consequently, this study aims to address the pressing issues of low seed fill rates and seed placement accuracy for rapeseed.

The objective of this study is to propose a shaped groove eyelet wheel seeder specifically designed for rapeseed planting, building upon the foundation of the traditional shaped groove eyelet wheel seeder. The conventionally shaped hole has been refined into two distinct components: a trapezoidal seed guide groove and a shaped groove, based on theoretical analysis and EDEM simulation tests. This enhancement seeks to augment seed aggregation capabilities, thereby increasing both seed loading efficiency and sowing precision. The operational performance and efficiency of the seeder are validated through subsequent bench tests, establishing a solid groundwork for the design of a precision seeder for rapeseed in the arid regions of northwest China.

2 Seed discharger working principle and theoretical analysis

2.1 Seed displacer working principle

The shaped groove eyelet wheel precision rapeseed planter is a collector-type seeding device, with its core structure outlined in Figure 1. The planter comprises several key components, including a housing, seed brush, seed guard plate, seed blocking plate, grooved wheel, fixing plate, seed unloading plate, forced sowing mechanism, sowing adjustment system, and a seed hopper. The operational principle of the planter is illustrated in Figure 2.

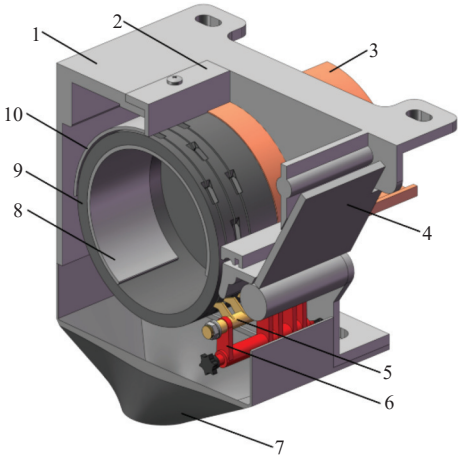

1. Shell 2. Seed brush 3. Seed baffle 4. Seed unloading plate 5. Forced seeding device 6. Seed feeding adjustment device 7. Funnel 8. Fixed plate 9. Shaped groove eyelet wheel 10. Seed protection board

Figure 1 Cutaway view of shaped groove eyelet wheel rapeseed precision seed dispenser

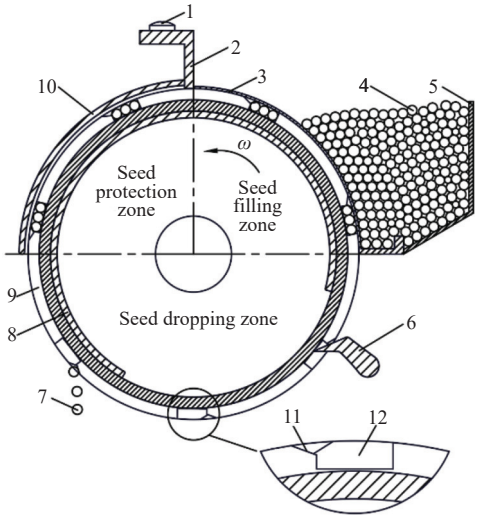

1. Self-tapping screw 2. Seed brush 3. Seed baffle 4. Seed cluster 5. Housing 6. Seed cleaning sheet 7. Rapeseed 8. Fixing plate 9. Shaped groove eyelet wheel 10. Seed protection board 11. Trapezoidal seed guide 12. Shaped groove

Figure 2 Working principle of shaped groove eyelet wheel

Prior to operation, the seed retention plate is adjusted to match the desired sowing rate. Seeds are then gravity-fed into the seed-filling area and guided into the shaped groove via the trapezoidal seed guide of the eyelet wheel. As the wheel rotates, it engages with the seed brush, which removes excess seeds, returning them to the filling zone[17]. The remaining seeds are carried by the rotating wheel, directed by the seed guard plate to the discharge point. However, due to variability in seed size, issues such as seed

accumulation or jamming may occur. To address this, a forced seed-feeding device[18] is integrated into the seed delivery area. This device features a spade-shaped seed-cleaning blade that inserts into the groove of the eyelet wheel, ensuring consistent seed discharge. Additionally, the blade clears seed debris and dust from the groove, facilitating smooth operation and consistent wheel rotation, even in challenging field conditions.

2.2 Analysis of the seed filling process in seed dischargers

The seed-filling process, which plays a pivotal role in determining the accuracy of the seeder[19], operates as a complex dynamic system influenced by multiple forces, including seed gravity, interactions within the seed population, and the forces acting between the seed's center of mass and the seed wheel. Its primary purpose is to efficiently extract target seeds from the population as the irregularly shaped groove wheel rotates, and subsequently guide them into the irregularly shaped groove to complete the filling process. This process comprises two critical stages: the detachment of target seeds from the seed mass and their subsequent deposition into the mold cavity.

During the operation of the seed discharger, the stacked seed population is disturbed by the rotational motion of the shaped eyelet wheel[20]. The seed layer closest to the wheel overcomes resistance from the upper layers and gravitational force through the support and friction provided by the wheel, causing the seeds to roll and slip. Throughout this process, kinetic and internal energy are continuously exchanged within the seed population, creating a dynamic state that facilitates the release of target seeds, allowing them to enter the shaped groove. Once the target seeds are separated from the population, they remain in a relatively stable state. As the shaped groove rotates beneath the target seed, the supporting force exerted by the wheel on the seed's center of mass is removed, causing the seed to slide into the aperture under the influence of combined forces, thereby initiating the seed-filling process.

In this study, the structural parameters of the traditional-shaped holes were improved, and the traditional rectangular seed guide groove was modified into a trapezoidal seed guide groove to enhance the seed filling efficiency of rapeseed. The trapezoidal seed guide groove has a larger spatial area, which can accommodate more seeds per unit time and has a higher seed filling efficiency. The trapezoidal structure facilitates the gathering, guiding, and extraction of the target seeds, providing a larger holding area that stabilizes the seeds as they flow through the seed guide slot, thereby avoiding jamming caused by the simultaneous filling of multiple seeds. Additionally, the trapezoidal seed guide groove encourages the target seeds to flow into the hole, overcoming the temporary 'arching' phenomenon that occurs when the seed's own gravity is less than the inter-seed friction, thus preventing leakage due to failure to slide within the shaped groove[21]. The movement of seeds in both the rectangular seed guide groove and the trapezoidal seed guide groove is illustrated in Figure 3.

3 Design of critical components

3.1 Basic parameters of rapeseed grains

The physical properties and basic parameters of the seeds exert a significant influence on the structural design of the seed displacer. The mean values of the triaxial dimensions (length, width, and height) of rapeseed grains measured in the experiment were 2.08±0.141 mm, 1.99±0.147 mm, and 1.89±0.198 mm, respectively. The mean particle size was determined to be 1.99 mm. The average sphericity of the seeds was 95.38%, with a water content of 5.31% and an average weight of 1000 grains being 4.71 g.

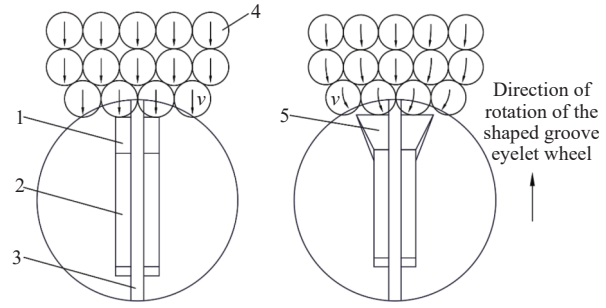

a. Rectangular seed-guide process b. Trapezoidal seed-guide process

1. Rectangular seed guide 2. Shaped holes 3. Seed cleaning grooves 4. Rapeseed grains 5. Trapezoidal seed guides

Figure 3 Partial diagram of the seed filling process of special-shaped hole

3.2 Design of eyelet wheel parameters

3.2.1 Determination of the diameter of the fovea wheel

The eyelet wheel is the key component of the seed dispenser[22], with its essential structural parameters including the diameter, the number of holes, and overall dimensions. Each hole comprises a trapezoidal seed guide groove and a shaped groove, as shown in Figure 4. According to reference[23], the seed filling time and the number of holes must adhere to the following equation:

$$\begin{cases} T = \dfrac{\pi\gamma}{180\omega} \\ \omega = \dfrac{2\pi n}{60} \\ \dfrac{v_m}{S} = \dfrac{zn}{60} \end{cases} \tag{1}$$

In the equation: T denotes the seed-filling time, s; γ represents the seed-filling angle, (°); ω is the angular velocity of the shaped groove wheel, rad/s; n indicates the rotational speed of the shaped groove wheel, r/min; z refers to the number of shaped cavities; S is the spacing between rapeseed grains, m; and v_m corresponds to the forward travel speed of the seeder, m/s.

The seed-filling angle γ refers to the angular range within which a single shaped groove can be effectively filled with seeds during the rotation of the shaped groove wheel. The magnitude of γ directly determines the effective filling duration per unit time, thereby influencing the qualified sowing rate. To determine γ, this study integrated the effective filling zone identified through EDEM simulations with measurements of the stable angular interval at which seeds successfully entered the shaped grooves under varying rotational speeds and inclination angles. The findings reveal that when γ is between 45° and 60°, the seed-filling qualification rate reaches its peak, while the rate of missed fillings is minimized. Consequently, γ=50° was selected as the optimal compromise between filling efficiency and seeding consistency. This choice is further corroborated by analysis of seed motion trajectories under the combined influence of gravity, frictional resistance, and centrifugal force, ensuring that the target seeds can consistently enter the cavities within the available time window.

$$T = \frac{\gamma z S}{360 v_m} \tag{2}$$

Equation (2), derived from Equation (1), reveals that under constant hole spacing and forward velocity, the seed filling time depends on the number of shaped grooves. A smaller diameter of the seed metering wheel corresponds to a reduced curvature radius, which in turn enhances its capacity to adsorb rapeseed. Conventionally, the diameter of such wheels is designed within the

range of 80-200 mm[24]. The seed metering wheel developed in this study was specifically engineered to comply with the designated row spacing specifications. The overall system configuration is constrained by the compact suspended layout illustrated in Figure 1, necessitating a minimization of the transmission system's spatial footprint while maintaining sufficient seed box volume. To improve the metering performance, the curvature radius of the wheel was reduced by 3 mm relative to standard designs, thereby enhancing seed adsorption and increasing filling efficiency. Taking into account both structural constraints and operational requirements, the final diameter of the seed metering wheel was determined to be 74 mm.

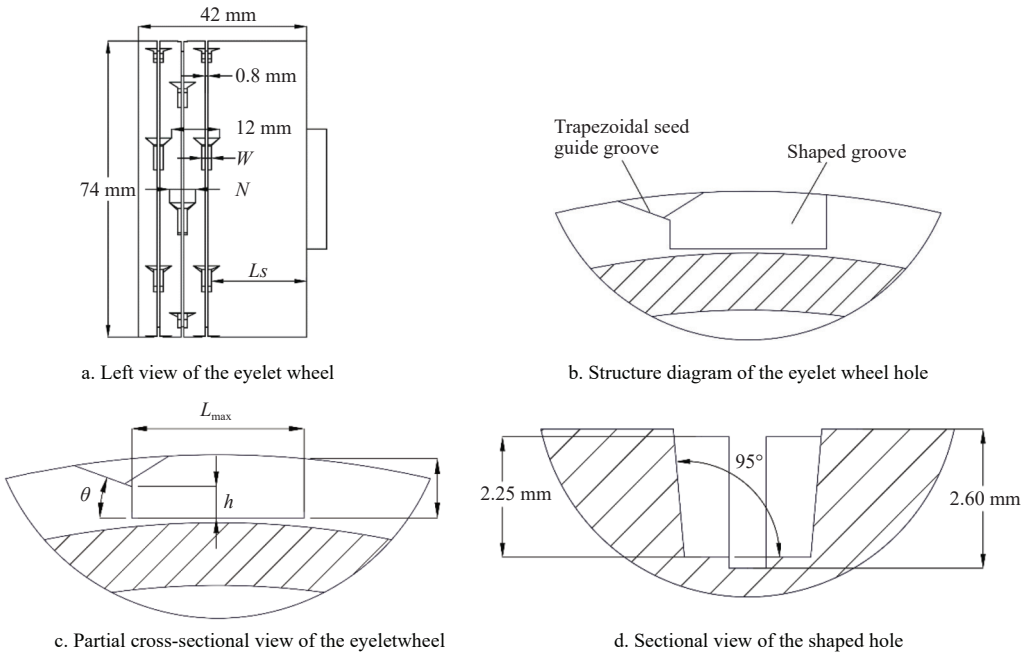

a. Left view of the eyelet wheel

b. Structure diagram of the eyelet wheel hole

c. Partial cross-sectional view of the eyeletwheel

d. Sectional view of the shaped hole

Figure 4 Distribution of shaped groove structures

3.2.2 Shaped groove design

The structural dimensions of the shaped groove are directly related to seed size, with the length, width, and height of the hole designated as L, W, and H, respectively. The inclination angle of the trapezoidal seed-guiding groove is represented by θ, and the width of the groove is defined as N. The depth of the seed storage area is denoted as h. Based on the physical characteristics of rapeseed, the design stipulates that each fossa hole accommodates (3±1) seeds, arranged in a single layer side by side when filled. To facilitate seed entry and discharge, the shaped grooves are molded into a trapezoidal form with an angle of 95.5°. Additionally, the trapezoidal seed guide grooves are configured at an angle of 20°, thereby enhancing the filling area for the guiding grooves. To accommodate three rapeseed grains within the aperture, the following equations must be satisfied:

$$\begin{cases} L_{\max} = 3a + k_l \\ W = b \times k_w \\ H = c \times k_h \\ h > \dfrac{1}{2}H \\ 1.5W_{\max} \le N \le 3W_{\min} \end{cases} \tag{3}$$

where, a represents the average length of rapeseed, mm; b denotes the average width of rapeseed, mm; c indicates the average height of rapeseed, mm; h signifies the depth of seed storage, mm; k_l is the length increment, ranging from 0.2 to 1.1 mm; k_w is the width increment, ranging from 0.9 to 1.2 mm; k_h is the height increment, ranging from 1.1 to 1.3 mm; and N represents the width of the trapezoidal seed guide grooves, mm.

Based on Equation (3) and the basic dimensions of rapeseed grains, the preliminary structural data of the shaped groove are determined as follows: $L_{\max}$=6.60 mm, W=2.35 mm, H=2.25 mm, h=1.50 mm, N=5.5 mm. The primary function of the seed guide groove is to facilitate the smooth entry and discharge of seeds into and out of the shaped aperture while minimizing seed damage during the process. The inclination angle θ of the groove must exceed the maximum static friction angle between the seed and the material of the shaped groove wheel. Experimental measurements determined this maximum static friction angle to be 18.7°. Therefore, to ensure proper seed filling and discharge, the condition θ>18.7° must be satisfied[19].

To mitigate seed coat detachment and the jamming phenomenon caused by multiple seeds entering the shaped hole due to vibrations during the operation of the seed planter, a forced sowing cleaning groove has been incorporated at the center of each row of shaped holes. Experimental measurements indicate that the average grain size of rapeseed is 1.99 mm, which is relatively small. Consequently, the width of the cleaning groove should not be excessive, to minimize stress on the seeds within the irregular groove, and it should not be overly deep to prevent excessive accumulation of debris that may be difficult to remove. Considering all relevant factors, the width of the cleaning groove has been established at 0.8 mm and the depth at 2.6 mm, thereby facilitating the subsequent removal of obstructed seeds.

3.2.3 Number and distribution of shaped grooves

The shaped groove is the core component of the eyelet wheel, and its quantity and spatial distribution directly determine the seed-filling efficiency of the seed-metering device. Based on the structural dimensions of the eyelet wheel and the requirements for precision sowing, the number and arrangement pattern of the shaped apertures per revolution were designed according to the following parameters: rapeseed intra-hole spacing S=0.15 m; typical rotational

speed of the seed metering wheel ranging from 10 to 50 r/min, with this study adopting n=20 r/min for calculation; and forward velocity of the seeder v_m=1 m/s. Based on these parameters, an equation was established to determine the required number of shaped apertures per revolution:

$$\begin{cases} \omega = \dfrac{2\pi n}{60} \\ z = \dfrac{60 v_m}{S n(1-\delta)} \end{cases} \tag{4}$$

where, ω is the angular velocity of the pulley, rad/s; n is the speed of rotation of the pulley, r/min; δ is the slip rate, usually 5%; v_m is the speed of travel of the unit, m/s; S is the spacing between plants, m; z is the number of holes in the pulley.

Equation (4) indicates that $z\geq21$. To ensure uniform filling, the number of holes is set to 21, with the holes evenly spaced and arranged in three rows with seven holes in each row. The distribution structure is shown in Figure 4a.

3.2.4 Kinematic analysis of the seed filling process

Seed-filling efficiency is a critical metric for evaluating the performance of a seed metering device. An optimally designed hole structure facilitates a more stable state for the seeds during the filling process[25]. When seeds enter the seed filling zone and come into contact with the hole, the filling process initiates, during which the target seeds undergo complex dynamic movements, gradually separating from the bulk population and entering the hole[26]. To analyze this movement, a single seed located at the edge of the irregular slot is selected. The force dynamics of this process are illustrated in Figure 5. A spatial coordinate system is established with the seed's center of mass as the origin, the x-axis along the tangential direction, the y-axis perpendicular to the exterior, and the z-axis perpendicular to the xoy plane passing through the center of the circular hole. As the seed wheel begins to rotate, the seed's center of mass is influenced by forces exerted by the surrounding population, its gravitational force, and the interaction with the seed wheel. Under the combined action of these forces, the seed enters the hole, completing the seed-filling process. Given the small size, high sphericity, and significantly lower Young's modulus of rapeseed compared to steel, they can be reasonably approximated as rigid, non-deformable spheres. Moreover, due to their negligible mass and velocity, air resistance during sowing operations can be safely disregarded.

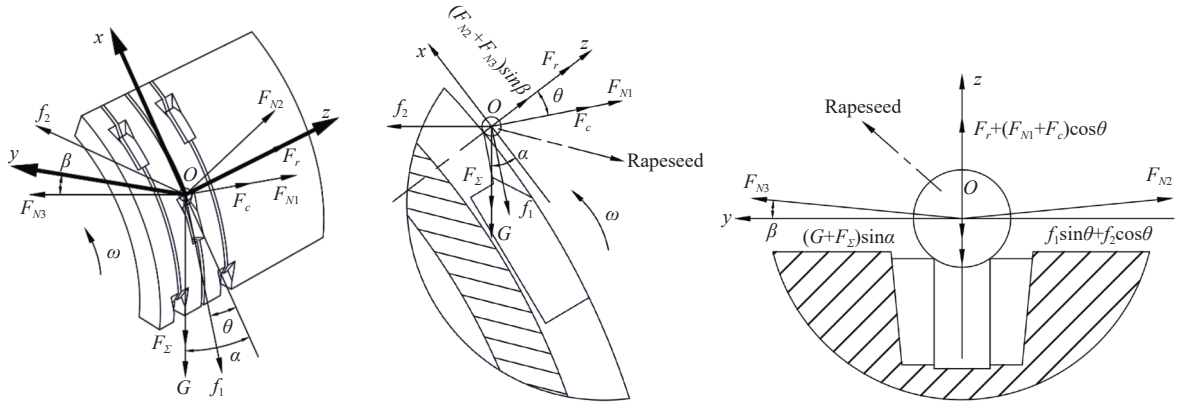

a. Spatial force analysis diagram of shaped groove

b. Planar force analysis diagram of shaped groove xoy

c. Planar force analysis diagram of shaped groove yoz

Figure 5 Force analysis diagram of the seed filling process of shaped groove

The seeds in the xoz and yoz planes are analyzed and the following equilibrium equations are established:

$$\begin{cases} (F_\Sigma + G)\sin\alpha + f_1\sin\theta + f_2\cos\theta - (F_c + F_{N1})\cos\theta - \\ \qquad F_r - (F_{N2}+F_{N3})\sin\beta = ma_z \\ (F_\Sigma + G)\cos\alpha + f_1\cos\theta + (F_c + F_{N1})\sin\theta - f_2\sin\theta = ma_x \\ F_{N2} = F_{N3} \\ f_1 = \mu F_{N1} \\ f_2 = \mu F_\Sigma \\ F_r = mR\omega^2 \\ F_c = 2mv\omega \end{cases} \tag{5}$$

where, F_{N1} represents the supporting force between the center of mass of the seed and the trapezoidal seed guide groove, N; F_{N2} and F_{N3} are the supporting forces between the center of mass of the seed and the left and right walls of the trapezoidal seed guide groove, N; F_r denotes the centrifugal force acting on the target seed, N; F_Σ is the resultant force exerted by the surrounding particles on the center of mass of the seed, N; F_c refers to the Coriolis force acting on the target seed, N; G is the gravitational force exerted on the target seed, N; f_1 represents the frictional force exerted by the sleeve wheel on the target seed, N, while f_2 is the frictional force exerted by the surrounding particles on the target seed, N; θ is the angle of inclination of the trapezoidal seed guide groove, measured, (°); α denotes the angle between the gravitational force and the tangent to the shaped groove wheel, (°); β is the angle between the left and right walls of the trapezoidal seed guide groove and the horizontal plane, (°); μ_1 and μ_2 represent the coefficients of friction between the target seed and the shaped groove wheel and the surrounding particles, respectively; a_z and a_x denote the accelerations of the target seed along the z-axis and x-axis, m/s^2.

From Equation (5), the resultant force acting during the seed filling process can be determined as follows:

$$\begin{cases} ma_z = \sqrt{f_1^2 + (f_2 - 2mv\omega - F_{N1})^2}\sin\left(\theta + \arctan\dfrac{f_2 - 2mv\omega - F_{N1}}{f_1}\right) + \\ \qquad (F_\Sigma + G)\sin\alpha - (F_{N2}+F_{N3})\sin\beta - mR\omega^2 \\ ma_x = \sqrt{f_1^2 + (2mv\omega + F_{N1} - f_2)^2}\sin\left(\theta + \arctan\dfrac{f_1}{2mv\omega + F_{N1} - f_2}\right) + \\ \qquad (F_\Sigma + G)\cos\alpha \end{cases} \tag{6}$$

From Equation (6), it is evident that the resultant force during the seed filling process is primarily influenced by the inclination

angle θ of the seed guide groove and the angular velocity ω of the shaped groove wheel. As the mold hole rotates into the seed-filling zone and makes contact with the seed population, a greater inclination angle of the seed guide groove increases the force components acting along the x- and z-axes on the target seed. This facilitates a balance between the forces exerted by the shaped groove wheel and the seed population during the filling process, ensuring a more stable transition of the seed into the shaped hole. However, if the inclination angle of the seed guide groove is excessively large, the effective length of the groove may be reduced, thereby compromising its seed-filling efficiency. Taking into consideration the previously measured maximum static friction angle between the seeds and the shaped groove wheel material, an initial inclination angle of 30° for the seed guide groove is selected.

3.2.5 Determination of the rotational speed of the eyelet wheel

The rotational speed significantly influences the operational efficiency of the seed dispenser[27]. During operation, the target seeds are driven into the shaped grooves under the combined effects of inter-seed forces, gravitational pull, and friction from the rotating eyelet wheel. If the wheel rotates too rapidly, the centrifugal force acting on the seeds surpasses their gravitational weight and population pressure. Additionally, the short duration of force application owing to the high rotational speed prevents seeds from effectively entering the shaped grooves, resulting in increased instances of missed sowing. To ensure efficient seed filling, the velocity dynamics during seed entry were analyzed. The seed-filling process can be decomposed into two components: uniform motion in the tangential direction and uniformly accelerated motion toward the center of rotation with an initial velocity of zero[28]. The analytical model is shown in Figure 6.

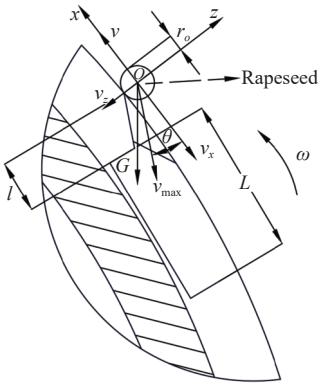

Figure 6 Speed distribution of the filling process of the shaped groove

Through the analysis, it is observed that the vertical displacement of the seed during the filling process is denoted as r_o, mm, while the displacement along the tangential direction is $L+l-r_o$, mm. In order for the seed to enter the cavity smoothly, the following conditions must be satisfied:

$$\begin{cases} r_o = \dfrac{1}{2}gt^2 \\ L + l - r_o = v_{\max} t \\ l = \dfrac{H-h}{\tan\theta} \end{cases} \tag{7}$$

where, r_o represents the radius of the seed, mm, g denotes the acceleration due to gravity, m/s^2, t signifies the seed filling time, s, and l refers to the length of the trapezoidal seed guide groove, mm. Additionally, $v_{\max}$ is the maximum rotational speed of the shaped groove wheel, m/s.

Based on Equation (7), it can be deduced that the permissible range for the maximum rotational speed of the shaped groove wheel is:

$$n_{\max} \le \frac{30}{\pi R}\left(L + \frac{H-h}{\tan\theta} - r_o\right)\sqrt{\frac{g}{2r_o}} \tag{8}$$

Given that R=37 mm, L=6.60 mm, H=2.25 mm, h=1.50 mm, and r_o=0.995 mm, the limiting speed of the seed wheel is determined to be 126.32 r/min, as derived from existing research [19] and Equation (8).

4 Discrete element simulation test and analysis

4.1 Simulation model building and simulation parameter determination

4.1.1 Simulation model building

In this investigation, “Longyou No. 19,” a double low rapeseed variety cultivated in Gansu Province, served as the experimental subject. The average moisture content of the rapeseed grains was determined to be 5.31% through drying tests. The Hertz-Mindlin (no-slip) contact mechanics model was employed to simulate the flow characteristics of the rapeseed[29]. A three-dimensional structural model of the seed meter was constructed using SolidWorks software, and after eliminating redundant non-contact components, it was imported into EDEM simulation software. The resulting simulation model of the seed meter is depicted in Figure 7.

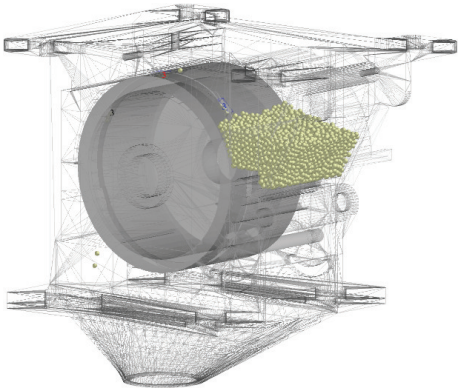

Figure 7 Simulation model of shaped groove fossa eye wheel

4.1.2 Setting of simulation parameters

During the operation of the seed meter, rapeseed primarily interacts with the shaped groove wheel, seed retaining plate, seed unloading plate, brush, and other seeds. The brush and seed unloading plate are predominantly composed of nylon, while the seed retaining plate is fabricated from PLA plastic, and the shaped groove wheel is constructed from photosensitive resin. The rapeseed used in this study belonged to the “Longyou 19” cultivar, cultivated in the Gansu region of China. The grains exhibited a high sphericity index (95.38%) and a moisture content of 5.31% (wet basis), with a mean thousand-seed weight of 4.71 g. Their three-dimensional morphological characteristics—length, width, and thickness—measured (2.08±0.141) mm, (1.99±0.147) mm, and (1.89±0.198) mm, respectively. Following systematic parameter calibration and validation against established literature [30], the intrinsic material properties and interparticle contact parameters were determined and are presented in Table 1.

4.2 One-factor simulation test

The above analysis reveals that several structural parameters of the shaped eyelet wheel, namely, the seed guide groove inclination angle, width of the trapezoidal guide groove, width of the shaped groove opening, and rotational speed of the eyelet wheel, exert a

Table 1 EDEM simulation contact parameters

Parameters	Rapeseed	Photosensitive resin	Nylon	PLA plastic	Source
Poisson's ratio	0.250	0.380	0.400	0.290	[29]
Density/kg·m^{-3}	1190	1130	1150	1110	[30]
Shear modulus/MPa	2.08×10^{2}	3.11×10^{3}	1.02×10^{2}	2.2×10^{2}	[29]
Collision restitution coefficient	0.397	0.655	0.600	0.639	[30]
Static friction coefficient	0.590	0.340	0.500	0.350	[30]
Rolling friction coefficient	0.046	0.060	0.100	0.064	[30]

significant influence on the seeding efficiency of the dispenser. To further refine the optimal parameter intervals and investigate their impact on seeding efficiency, a single-factor simulation experiment was conducted to assess the seed collection and filling performance of the device[31]. The test factors included the inclination angle θ of the seed guide groove, the width N of the trapezoidal guide groove, the width W of the shaped groove, and the rotational speed ω of the shaped groove wheel, with fixed values of 30°, 5 mm, 2.35 mm, and 25 r/min, respectively. The performance indicators were the pass rate of seed filling per hole (Y_1: (3±1) seeds/hole), the reseeding rate (Y_2: 5 or 6 seeds/hole), and the missed seeding rate (Y_3: 0 or 1 seed/hole). The test simulation ran for 15 seconds, and the filling status of 105 holes was analyzed after five rotations of the shaped groove wheel. The pass, reseeding, and missed seeding rates were calculated, and the experiment was repeated three times with average values recorded.

During the simulation, the seed-gathering efficiency of the trapezoidal guide slot and the seed-filling capacity of the shaped groove were analyzed over different periods. As depicted in Figure 2, when the seeds enter the filling area, the seed population fluctuates. Once the hole rotates to the position of the seed brush, seed filling is essentially complete, and the number of seeds in the hole stabilizes. Therefore, the number of seeds passing through the seed guide groove in the filling area serves as a measure of the gathering efficiency of the trapezoidal seed guide groove. In contrast, the stable number of seeds in the hole when it reaches the seed protection area is used to evaluate seed filling efficiency.

4.2.1 Angle of inclination of trapezoidal seed guide

Based on the analysis presented in Section 2.2.2 of this study, a simulation was conducted with the inclination angle θ of the seed guide groove set at 20°, 30°, 40°, and 90° (the latter representing the absence of a seed guide groove). To facilitate statistical analysis of the number of seeds filled in the trapezoidal and rectangular seed guide grooves, the EDEM post-processing Geometry Bin function was employed. This function allowed the creation of two spatial geometric bodies, A and B, which enveloped the trapezoidal seed guide groove and the shaped groove, respectively, and rotated in unison with the shaped hole. Geometric body A had dimensions of 6.8 mm in length, 3 mm in width, and 4 mm in height, while geometric body B measured 2.5 mm in length, 4.6 mm in width, and 2 mm in height. The bottom surfaces of both A and B were parallel to the tangent direction of the shaped groove wheel. Their spatial arrangement is illustrated in Figure 8. To enhance the efficiency of the experiment, the analysis focused solely on the seed-filling performance of the middle column of the three columns in the shaped groove wheel. To ensure statistical robustness, seed counts from three consecutive holes were recorded after five rotations of the shaped groove wheel, and the average value was calculated. The results of the simulation test are provided in Table 2.

As indicated in Table 2, the average number of seeds passing through the trapezoidal seed guide groove within the same period is higher, demonstrating its superior seed-filling performance. The trapezoidal structure, characterized by a larger spatial volume and a wider design at the top and narrower at the bottom, provides enhanced flow dynamics. This structure improves seed collection, guiding, and extraction of target seeds, thereby outperforming traditional seed guide grooves in filling efficiency.

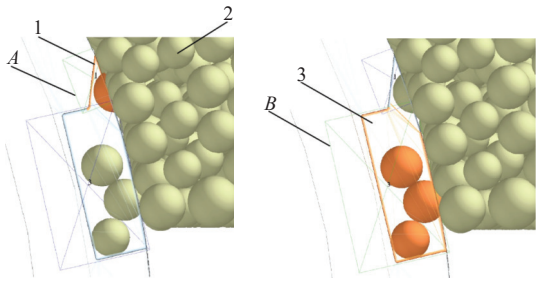

a. Type A spatial geometry b. Type B spatial geometry

1. Trapezoidal seed guide groove; 2. Seed population; 3. Special-shaped slot

Figure 8 Space geometry distribution

Table 2 Simulation results for different inclination angles of seed filling

Inclination/(°)	Number	Rectangular seed guide groove			Trapezoidal seed guide groove		
		Filling rate/%	Average/%	Coefficient of variation/%	Filling rate/%	Average/%	Coefficient of variation/%
20	1	0.071	0.051	0.348	0.081	0.057	0.367
	2	0.040			0.040		
	3	0.041			0.051		
30	1	0.070	0.047	0.446	0.040	0.054	0.217
	2	0.030			0.061		
	3	0.040			0.061		
40	1	0.030	0.023	0.247	0.020	0.030	0.333
	2	0.020			0.040		
	3	0.020			0.030		

Based on these findings, the simulation pass rate for the trapezoidal seed guide groove at various inclination angles was statistically analyzed, and the results are summarized in Table 3. As shown, the seed-filling performance of the shaped groove decreases as the inclination angle increases. At lower inclination angles, the seed guide groove has a larger spatial volume and better seed-gathering ability, leading to a higher reseeding rate. However, at larger inclination angles, the seed guide groove loses its guiding effect, which contributes to an increased rate of missed seeds in the shaped groove.

This study utilized the EDEM post-processing function and Origin 2018 software to examine the changes in the normal force and kinetic energy between the seed population and the shaped groove at different inclination angles. As illustrated in Figure 9, when the inclination angle of the seed guide groove is 90° (i.e., without a seed guide groove), both the normal force and dynamic fluctuations between the population and the shaped groove are significantly higher, resulting in poorer stability. This is because, in the absence of a seed guide groove, the shaped hole loses its ability to efficiently gather and drain seeds, causing greater disorder in the seed-filling process. When the inclination angle of the seed guide groove ranges between 20° and 40°, stability between the population and the shaped groove improves significantly, indicating that a seed guide groove with a certain inclination angle reduces the interaction between the population and the shaped hole, thus facilitating smoother seed filling.

Table 3 Simulation results of pass rate for different inclination angles

Inclination/(°)	Number	Qualified seeding rate/%			Reseeding rate/%			Missed seeding rate/%		
		Simulation	Average	Coefficient of variation	Simulation	Average	Coefficient of variation	Simulation	Average	Coefficient of variation
20	1	90.48	90.48	2.11	7.62	6.98	7.86	1.90	2.54	78.08
	2	92.38			6.67			0.95		
	3	88.57			6.67			4.76		
30	1	95.24	93.97	1.55	2.86	4.76	40.02	1.90	1.27	43.19
	2	92.38			6.67			0.95		
	3	94.29			4.76			0.95		
40	1	89.52	89.52	2.13	2.86	2.86	33.39	7.62	7.62	37.53
	2	91.43			3.81			4.76		
	3	87.62			1.90			10.48		
90	1	79.05	78.10	3.23	5.71	6.03	24.16	15.24	15.87	24.26
	2	80.00			7.62			12.38		
	3	75.24			4.76			20.00		

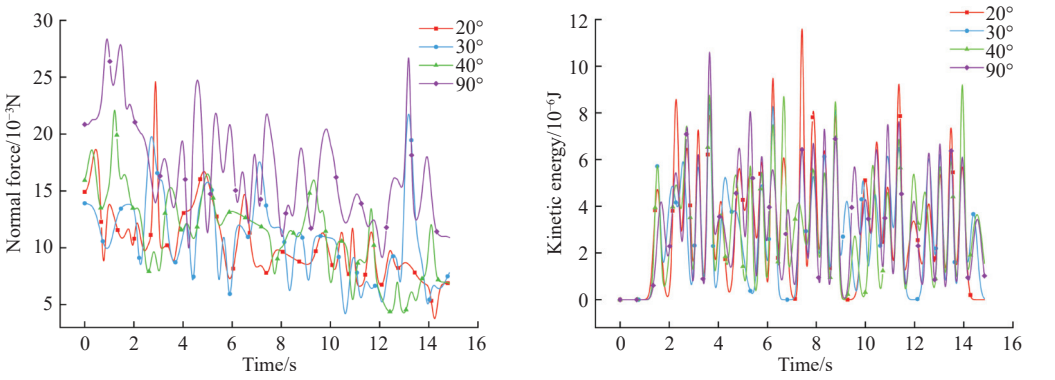

a. Variation of normal force between populationswith different inclination angles and the shaped groove wheel

b. Variation of kinetic energy between populations with different inclination angles and the shaped groove wheel

Figure 9 Influence of different inclination angles of seed guides on seed populations

By correlating the results from Tables 2 and 3, it can be observed that as the inclination angle of the seed guide groove increases, the seed-filling efficiency of the shaped groove initially improves and then declines. At smaller angles, the larger contact area allows for better seed collection, but an excessively large area increases the reseeding rate. Therefore, the inclination angle should not be too small. When the inclination angle is excessively large, the guiding effect of the seed groove on the seed population diminishes, and the disturbance caused by the shaped groove to the seed flow weakens. As a result, seed accumulation occurs, leading to an increased rate of missed sowing. Therefore, when the inclination angle θ was set to 30°, the seed filling performance was the most stable, exhibiting the highest qualification rate and a relatively low coefficient of variation.

4.2.2 Width of trapezoidal seed guide

The seed-filling performance of trapezoidal seed guide grooves with widths of 4.5 mm, 5.5 mm, 6.5 mm, and 7.5 mm is presented in Table 4.

Table 4 Simulation results of pass rate for different inclination angles

Width/mm	Number	Qualified seeding rate/%			Reseeding rate/%			Missed seeding rate/%		
		Simulation	Average	Coefficient of variation	Simulation	Average	Coefficient of variation	Simulation	Average	Coefficient of variation
4.5	1	91.43	91.43	2.08	1.90	2.86	57.74	6.67	5.71	16.73
	2	93.33			1.90			4.76		
	3	89.52			4.76			5.71		
5.5	1	97.14	96.51	1.14	0.00	0.63	87.06	2.86	2.86	33.39
	2	95.24			0.95			3.81		
	3	97.14			0.95			1.90		
6.5	1	92.38	93.97	1.54	5.71	4.76	34.57	1.90	1.27	86.60
	2	95.24			2.86			1.90		
	3	94.29			5.71			0.00		
7.5	1	86.67	87.62	1.88	10.48	9.52	10.03	2.86	2.86	33.39
	2	89.52			8.57			1.90		
	3	86.67			9.52			3.81		

As shown in Table 4, the width of the trapezoidal guide groove significantly affected the seed-filling efficiency of the shaped groove. A wider groove results in a larger spatial area within the groove, allowing more seeds to pass through per unit time. With increasing groove width, the reseeding rate of the shaped groove gradually increased, whereas the rate of missed seedings decreased.

According to Figure 10, when the groove width is small, both the disturbance and guiding effects on the seed population are limited to a certain extent. Under the influence of gravity, the normal force and kinetic energy between the target seeds and the shaped groove increase, making the seeds more prone to crushing, which ultimately reduces the seeding efficiency. As the groove width increased, the stability of the normal force and kinetic energy between the seed population and eyelet wheel initially improved and then declined. This indicates that an excessive width leads to more seeds coming into contact with the shaped groove, intensifying the interactions between the seed population and the wheel. The resulting increase in energy exchange may cause seed accumulation in the shaped groove, hindering seed discharge and reducing seeding efficiency. Considering the interaction effects among the parameters in subsequent experiments, the optimal width of the trapezoidal guide groove was determined to be 4.5~6.5 mm.

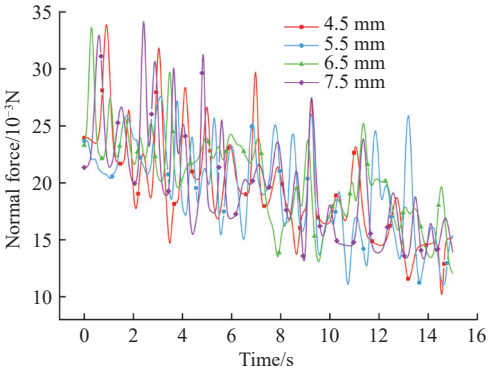

a. Variation of normal force between populations with different inclination angles and the shaped groove wheel

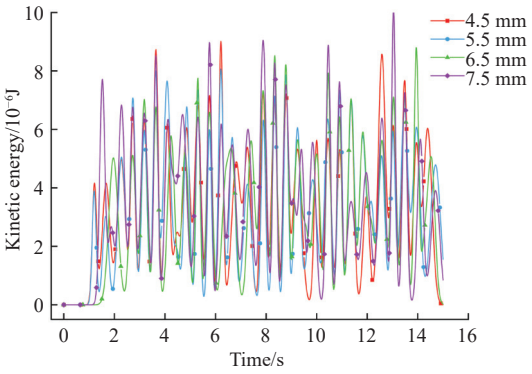

b. Variation of kinetic energy between populations with different inclination angles and the shaped groove wheel

Figure 10 Effect of different trapezoidal seed guide widths on seed populations

4.2.3 Width of shaped groove

The width of the shaped groove plays a crucial role in determining the filling efficiency of rapeseed kernels. In this study, the widths of the shaped grooves were set to 2.20, 2.35, 2.50, and 2.65 mm, respectively. The results of these tests are presented in Table 5.

As shown in Table 5, an increase in the width of the shaped groove opening led to a gradual decrease in the rate of missed seeding, whereas the reseeding rate increased. The qualification rate first increased and then decreased. As shown in Figure 11, when the groove width is relatively narrow, the normal force and kinetic energy between the seed population and eyelet wheel are relatively

Table 5 Simulation results of different shaped notch width pass rate

Width/mm	Number	Qualified seeding rate/%			Reseeding rate/%			Missed seeding rate/%		
		Simulation	Average	Coefficient of variation	Simulation	Average	Coefficient of variation	Simulation	Average	Coefficient of variation
2.20	1	91.43	93.02	2.96	0.95	0.63	86.60	7.62	6.35	48.18
	2	96.19			0.95			2.86		
	3	91.43			0.00			8.57		
2.35	1	94.29	95.24	0.99	1.90	2.54	21.82	3.81	2.22	65.61
	2	95.24			2.86			1.90		
	3	96.19			2.86			0.95		
2.50	1	92.38	91.43	1.81	5.71	6.66	37.81	1.90	1.90	50.18
	2	89.52			9.52			0.95		
	3	92.38			4.76			2.86		
2.65	1	82.86	85.71	3.33	11.43	10.48	9.12	5.71	3.81	50.04
	2	85.71			10.48			3.81		
	3	88.57			9.52			1.90		

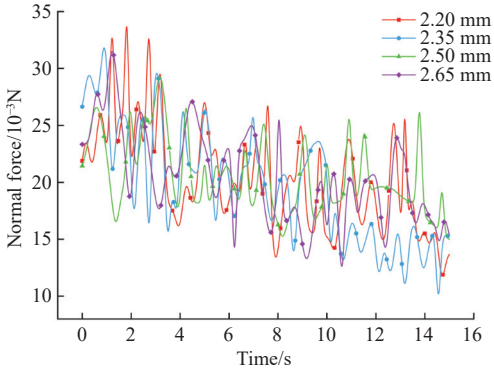

a. Variation of normal force with different shaped groove widths and the shaped groove wheel

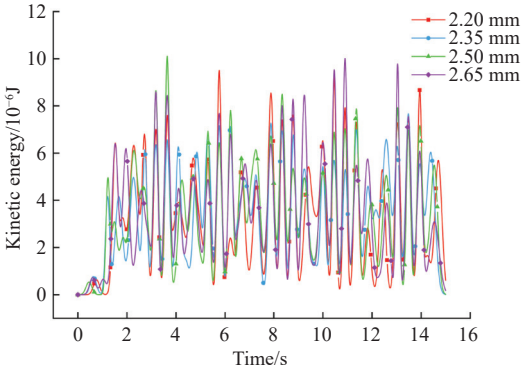

b. Variation of kinetic energy with different shaped groove widths and the nesting eyelet wheel

Figure 11 Impact of different alien slot widths on the population

high, indicating that an excessively narrow groove imposes substantial stress on the seeds, increasing the risk of mechanical damage. When the groove width reached 2.65 mm, both the normal force and kinetic energy were reduced, and the system demonstrated good stability. However, the accompanying increase in the reseeding rate suggests that an excessively wide groove is undesirable. A comprehensive analysis indicated that the optimal width of the shaped groove opening was within the range of 2.20~2.50 mm.

4.2.4 Rotation speed of the eyelet wheel

The rotational speed of the shaped groove exerts a notable influence on the seed-filling performance. In this study, the shaped groove speeds were set at 15, 20, 25, and 30 r/min, respectively. The corresponding test results are presented in Table 6.

Table 6 Simulation results of qualification rates for different rotational speeds

Rotational speed /r·min^{-1}	Number	Qualified seeding rate/%			Reseeding rate/%			Missed seeding rate/%		
		Simulation	Average	Coefficient of variation	Simulation	Average	Coefficient of variation	Simulation	Average	Coefficient of variation
15	1	91.43	93.33	2.70	3.81	3.81	24.93	4.76	2.86	66.69
	2	96.19			2.86			0.95		
	3	92.38			4.76			2.86		
20	1	97.14	95.56	1.52	0.95	1.90	86.75	1.90	2.54	43.47
	2	95.24			0.95			3.81		
	3	94.29			3.81			1.90		
25	1	89.52	91.43	2.08	2.86	2.86	33.43	7.62	5.72	44.07
	2	91.43			1.90			6.67		
	3	93.33			3.81			2.86		
30	1	81.90	83.81	2.27	3.81	3.81	50.04	14.29	12.38	15.38
	2	85.71			1.90			12.38		
	3	83.81			5.71			10.48		

As shown in Table 6, the seed-filling efficiency of the shaped groove remained relatively stable at lower rotational speeds. The reduced speed provided sufficient buffering time for the seeds, thereby enhancing the reseeding rate. However, with increasing rotational speed, the time available for seed filling decreases, resulting in a higher incidence of missed seedings. As shown in Figure 12, the rapid rotation of the shaped groove shortens the contact duration between the seed population and the groove, thereby diminishing the frequency of interaction events. Consequently, the normal force between the target seeds and the shaped groove exhibited a declining trend. Further analysis revealed that higher rotational speeds significantly increased the disturbance within the seed population and induced greater fluctuations in the kinetic energy. This suggests that excessive rotational speed may increase the likelihood of seed breakage and ultimately reduce overall sowing efficiency. Considering both seed-filling stability and mechanical performance, the optimal rotational speed for the shaped groove was determined to be within the range of 15-25 r/min.

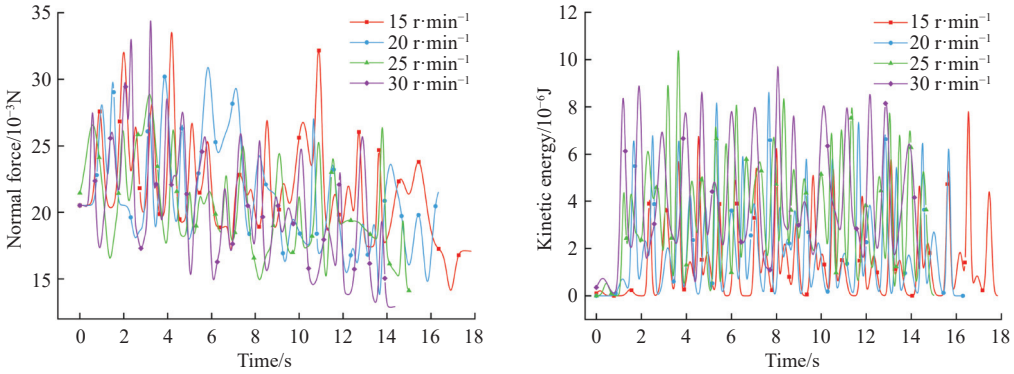

a. Variation of normal force with different rotational speeds and the shaped groove wheel

b. Variation of kinetic energy with different rotational speeds and the nesting eyelet wheel

Figure 12 The impact of different rotational speeds on the population

4.3 Quadratic regression orthogonal rotation combination simulation test

4.3.1 Pilot program

To investigate the effects of the inclination angle of the seed guide groove, the width of the trapezoidal seed guide groove, the width of the special-shaped slot, and the rotational speed of the shaped groove on the operational performance of the seed metering device, a quadratic regression orthogonal rotation combination simulation test was conducted based on the results of the individual factor simulations. The experimental factor coding is presented in Table 7, while the design scheme and corresponding analysis results are listed in Table 8. In these tables, X_1, X_2, X_3, and X_4 represent the coded values for the experimental factors, with Y_1 (qualified seeding rate), Y_2 (reseeding rate), and Y_3 (missed seeding rate) serving as the performance indicators.

Table 7 Test factors and levels

Horizontal	Factors			
	Seed guide groove inclination angle/(°)	Trapezoidal seed guide groove width/mm	Shaped groove width/mm	Nesting eye wheel speed/ r·min^{-1}
–1	20	4.5	2.20	15
0	30	5.5	2.35	20
1	40	6.5	2.50	25

Table 8 Experimental design and experimental results

Number	X_1	X_2	X_3	X_4	Y_1/%	Y_2/%	Y_3/%
1	20.00	4.50	2.35	20.00	90.48	7.62	1.90
2	40.00	4.50	2.35	20.00	91.43	0.95	7.62
3	20.00	6.50	2.35	20.00	92.38	5.71	1.90
4	40.00	6.50	2.35	20.00	87.62	4.76	7.62
5	30.00	5.50	2.20	15.00	91.43	5.71	2.86
6	30.00	5.50	2.50	15.00	85.71	11.43	2.86
7	30.00	5.50	2.20	25.00	80.95	3.81	15.24
8	30.00	5.50	2.50	25.00	86.67	4.76	8.57
9	20.00	5.50	2.35	15.00	89.52	8.57	1.90
10	40.00	5.50	2.35	15.00	86.67	8.57	4.76
11	20.00	5.50	2.35	25.00	87.62	2.86	9.52
12	40.00	5.50	2.35	25.00	83.81	0.95	15.24
13	30.00	4.50	2.20	20.00	90.48	2.86	6.67
14	30.00	6.50	2.20	20.00	89.52	3.81	6.67
15	30.00	4.50	2.50	20.00	91.43	5.71	2.86
16	30.00	6.50	2.50	20.00	88.57	9.52	1.90
17	20.00	5.50	2.20	20.00	92.38	5.71	1.90
18	40.00	5.50	2.20	20.00	86.67	3.81	9.52
19	20.00	5.50	2.50	20.00	87.62	10.48	1.90
20	40.00	5.50	2.50	20.00	86.67	5.71	7.62
21	30.00	4.50	2.35	15.00	92.38	5.71	1.90
22	30.00	6.50	2.35	15.00	90.48	7.62	1.90
23	30.00	4.50	2.35	25.00	86.67	1.90	11.43
24	30.00	6.50	2.35	25.00	90.48	1.90	7.62
25	30.00	5.50	2.35	20.00	91.43	2.86	5.71
26	30.00	5.50	2.35	20.00	90.48	4.76	4.76
27	30.00	5.50	2.35	20.00	91.43	3.81	4.76
28	30.00	5.50	2.35	20.00	90.48	3.81	5.71
29	30.00	5.50	2.35	20.00	89.52	5.71	4.76

4.3.2 Analysis of test results

The Design-Expert 13 software was utilized to simulate and analyze the experimental design. Three simulation tests were conducted for each group, and the average values were computed. The experimental design and corresponding results are presented in Table 8.

4.3.3 Regression equation and significance test

The test results were analyzed employing the Box-Behnken central composite design, leading to the derivation of quadratic polynomial regression models for the qualified rate, reseeding rate, and missed seeding rate from the simulation tests, which are presented as follows:

$$\begin{cases} Y_1 = 90.67 - 1.43X_1 - 0.3183X_2 - 0.3967X_3 - 1.67X_4 - 1.43X_1X_2 + \\ \quad 1.19X_1X_3 - 0.24X_1X_4 - 0.475X_2X_3 + 1.43X_2X_4 + 2.86X_3X_4 - \\ \quad 1.13X_1^2 + 1.25X_2^2 - 1.72X_3^2 - 2.44X_4^2 \\ Y_2 = 4.19 - 1.35X_1 + 0.7142X_2 + 1.83X_3 - 2.62X_4 + 1.43X_1X_2 - \\ \quad 0.7175X_1X_3 - 0.4775X_1X_4 + 0.715X_2X_3 - 0.4775X_2X_4 - \\ \quad 1.19X_3X_4 + 0.6825X_1^2 - 0.2712X_2^2 + 1.63X_3^2 + 0.4438X_4^2 \\ Y_3 = 5.14 + 2.78X_1 - 0.3975X_2 - 1.43X_3 + 4.29X_4 - 0.475X_1X_3 + \\ \quad 0.715X_1X_4 - 0.24X_2X_3 - 0.9525X_2X_4 - 1.67X_3X_4 + 0.4433X_1^2 - \\ \quad 0.9829X_2^2 + 0.0896X_3^2 + 1.99X_4^2 \end{cases} \quad (9)$$

Through regression analysis of variance, it was determined that the regression model for the qualified rate exhibits a significance level of $p<0.01$, indicating extreme significance. The coefficient of determination (R^2=0.9139) for this model approaches 1, reflecting a high degree of reliability. As indicated in Table 9, the lack of fit item (p=0.1975) is not significant, suggesting that no other factors exert an influence on the qualified rate. After eliminating insignificant factors and refitting the regression equation for the qualified rate, the following expression is obtained:

$$Y_1 = 90.67 - 1.43X_1 - 1.67X_4 - 1.43X_1X_2 + 1.43X_2X_4 + 2.86X_3X_4 - 1.13X_1^2 + 1.25X_2^2 - 1.72X_3^2 - 2.44X_4^2 \quad (10)$$

Table 9 Regression equation variance analysis table

Source of variance	Qualified seeding rate Y_1				Reseeding rate Y_2				Missed seeding rate Y_3			
	Sum of squares	Degrees of freedom	F-value	p-value	Sum of squares	Degrees of freedom	F-value	p-value	Sum of squares	Degrees of freedom	F-value	p-value
Model	194.98	14	10.61	<0.0001	191.36	14	12.93	<0.0001	396.44	14	25.51	<0.0001
A	24.45	1	18.63	0.0007**	21.87	1	20.69	0.0005**	92.74	1	83.54	<0.0001**
B	1.22	1	0.9266	0.3521	6.12	1	5.79	0.0305*	1.90	1	1.71	0.2123
C	1.89	1	1.44	0.2503	39.97	1	37.81	<0.0001**	24.51	1	22.08	0.0003**
D	33.30	1	25.37	0.0002**	82.32	1	77.88	<0.0001**	220.51	1	198.63	<0.0001**
AB	8.15	1	6.21	0.0259*	8.18	1	7.74	0.0147*	0.0000	1	0.0000	1.0000
AC	5.66	1	4.32	0.0566	2.06	1	1.95	0.1845	0.9025	1	0.8129	0.3825
AD	0.2304	1	0.1756	0.6816	0.9120	1	0.8628	0.3687	2.04	1	1.84	0.1962
BC	0.9025	1	0.6877	0.4209	2.04	1	1.93	0.1860	0.2304	1	0.2075	0.6557
BD	8.15	1	6.21	0.0259*	0.9120	1	0.8628	0.3687	3.63	1	3.27	0.0921
CD	32.72	1	24.93	0.0002**	5.69	1	5.38	0.0360*	11.12	1	10.02	0.0069**
A^2	8.24	1	6.28	0.0252*	3.02	1	2.86	0.1130	1.27	1	1.15	0.3020
B^2	10.21	1	7.78	0.0145*	0.4773	1	0.4515	0.5126	6.27	1	5.64	0.0323*
C^2	19.26	1	14.68	0.0018**	17.34	1	16.40	0.0012**	0.0521	1	0.0469	0.8317
D^2	38.52	1	29.35	<0.0001**	1.28	1	1.21	0.2902	25.77	1	23.22	0.0003**
Residual	18.37	14	-	-	14.80	14	-	-	15.54	14	-	-
Misfit term	15.82	10	2.48	0.1975	10.10	10	0.8613	0.6161	14.46	10	5.34	0.0603
Error	2.55	4	-	-	4.69	4	-	-	1.08	4	-	-
Sum	213.36	28	-	-	206.16	28	-	-	411.98	28	-	-

Noe: The symbol ** denotes items of extreme significance ($p<0.01$), while * indicates items of significance ($p<0.05$).

From Equation (10), it is evident that the factors affecting the qualification rate are primarily the rotation speed of the shaped groove and the inclination angle of the seed guide groove. Conversely, the width of the trapezoidal seed guide groove and the width of the special-shaped notch do not significantly impact the qualification rate.

The regression analysis of variance further reveals that the regression model for the reseeding rate also achieves a significant level of $p<0.01$, which is extremely significant. The coefficient of determination (R^2=0.9282) for this model similarly approaches 1, indicating robust reliability. According to Table 9, the lack of fit item (p=0.6161) is not significant, demonstrating that no other factors influence the reseeding rate. After dismissing insignificant variables and refitting the regression equation for the reseeding rate, it is derived:

$$Y_2 = 4.19 - 1.35X_1 + 0.7142X_2 + 1.83X_3 - 2.62X_4 + 1.43X_1X_2 - 1.19X_1X_3 + 1.63X_3^2 \quad (11)$$

From Equation (11), it is apparent that the factors influencing the reseeding rate are ranked as follows: the rotation speed of the shaped groove, the width of the special-shaped slot, the inclination angle of the seed guide slot, and the width of the trapezoidal slot.

Lastly, regression analysis indicates that the model for the missed seeding rate yields a significant level of $p<0.01$, which is again extremely significant. The coefficient of determination (R^2=0.9623) for this model is also close to 1, affirming its high reliability. As shown in Table 9, the lack of fit item (p=0.0603) is not significant, indicating no additional factors affect the missed seeding rate. Following the removal of insignificant factors and the subsequent refitting of the regression equation for the missed seeding rate, it is arrived at:

$$Y_3 = 5.14 + 2.78X_1 - 1.43X_3 + 4.29X_4 - 1.67X_3X_4 - 0.9829X_2^2 + 1.99X_4^2 \quad (12)$$

An analysis of the regression coefficients from Equation (12) reveals that the order of influence on the missed seeding rate is determined by the rotation speed of the shaped groove, the inclination angle of the seed guide groove, and the width of the special-shaped notch, with the width of the trapezoidal seed guide groove showing no significant influence on the missed seeding rate.

4.3.4 Impact of factors on pass rate

The quadratic regression model for the response variables derived from the experiment was analyzed using Design-Expert 13 software. The response surfaces depicting the effects of the inclination angle of the seed guide groove, the width of the trapezoidal seed guide groove, the width of the special-shaped groove, and the rotation speed of the shaped groove on the qualified rate are presented in Figure 13. In this analysis, two of the influencing factors were held constant at the zero level, allowing for an examination of the interaction effects between the remaining two variables on the qualified rate.

As illustrated in Figure 13a, when the width of the shaped groove is set to 2.35 mm and the rotation speed of the shaped groove is 20 r/min, the qualified rate exhibits a gradual decline with increasing width and inclination angle of the trapezoidal seed guide groove. The qualified rate reaches its maximum when the width approaches 4.5 mm and the inclination angle nears 30°. As shown in Figure 13b, the highest qualification rate was achieved when the width of the trapezoidal seed guide groove ranged from 5 to 5.5 mm and the rotational speed of the eyelet wheel was between 21 and 23 r/min. Figure 13c indicates that, at a 30° inclination angle of the seed guide groove and a trapezoidal seed guide groove width of 5.5 mm, an increase in the width of the irregular groove leads to a swift rise in the qualified rate, which subsequently stabilizes; however, as the rotation speed of the shaped groove increases, the qualified rate gradually decreases. The maximum qualified rate occurs when the shaped groove width lies between 2.26 and 2.38 mm and the rotation speed is maintained between 19 and 23 r/min.

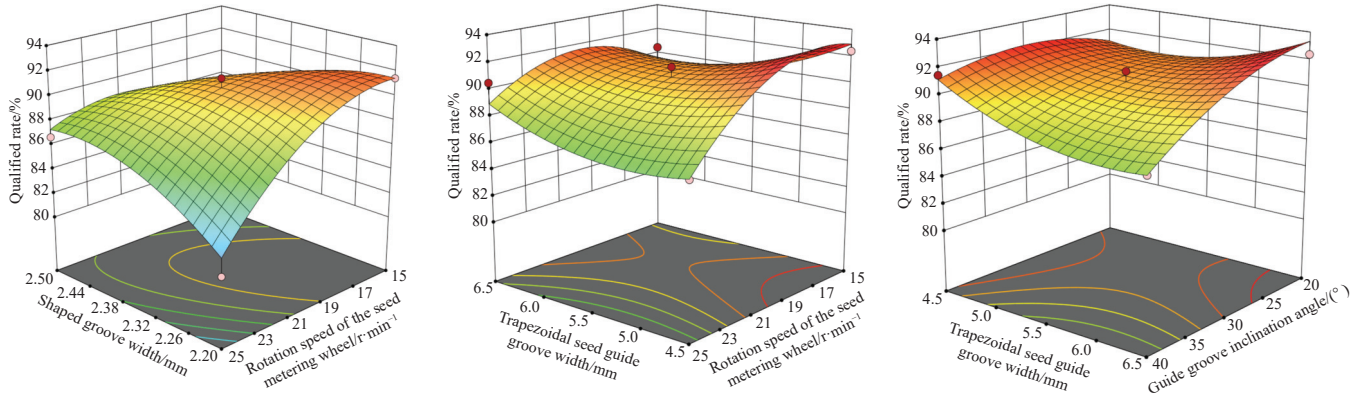

a. $Y_1=f(0, 0, X_3, X_4)$ b. $Y_1=f(0, X_2, 0, X_4)$ c. $Y_1=f(X_1, X_2, 0, 0)$

Figure 13 Effect of factor interactions on the qualification rate

4.3.5 Optimization and experimental validation of operating parameters

Each factor and its interactions significantly influence the seeding performance of the irregular shaped groove seed metering device. To enhance the qualified rate of rapeseed seeding, it is imperative to optimize parameters such as the inclination angle of the seed guide groove, the width of the trapezoidal seed guide groove, the width of the irregular groove, and the rotation speed of the shaped groove to ensure their harmonious interaction for optimal seed filling performance.

In both bench and field tests, the qualified rate of each hole serves as a critical determinant for stable seed production. Although reseeding can compensate for seed loss resulting from missed seeding, thereby promoting uniformity in seeding density, it is essential to minimize the missed seeding rate, with the reseeding rate being a secondary concern. The performance index for the seed meter stipulates that the qualified rate of seeds in each hole must exceed 80%, the reseeding rate must remain below 15%, and the missed seeding rate must be under 5%. To ascertain the optimal operating parameters of the seed meter, a regression mathematical

model will be established based on the boundary conditions of the experimental factors, with the objective function and constraints as follows:

$$F_{max} = Y_1 - Y_2 - Y_3 \tag{13}$$

$$\text{s.t.} \begin{cases} Y_1 > 80\% \\ Y_2 < 5\% \\ Y_3 < 15\% \\ 20^\circ \le X_1 \le 40^\circ \\ 4.5\ \text{mm} \le X_2 \le 6.5\ \text{mm} \\ 2.20\ \text{mm} \le X_3 \le 2.50\ \text{mm} \\ 15\ \text{r/min} \le X_4 \le 25\ \text{r/min} \end{cases} \tag{14}$$

The optimization of the objective function was performed using Design-Expert 13 software. The resulting optimal parameters included a seed guide groove inclination angle of 20°, a trapezoidal seed guide groove width of 6.5 mm, a shaped groove width of 2.21 mm, and an eye wheel rotation speed of 19.10 r/min. Under these conditions, the qualified rate of seed per hole was 94.17%, the reseeding rate was 3.92%, and the missed seeding rate was 1.90%.

To validate the reliability of these optimization results, the optimal parameter combination was used to conduct five repeated bench tests, and the average values were recorded. The test material comprised "Longyou No. 19" rapeseed, and the photosensitive resin shaped groove wheel, manufactured using a light-curing 3D printer (Figure 14), was installed on the JPS-12 computer vision seeding device test bench for performance evaluation. The test results, shown in Table 10, indicate a qualified rate of 90.17%, a reseeding rate of 5.36%, a missed seeding rate of 4.47%, and a breakage rate of 1.02%. Owing to experimental constraints including mechanical vibration, seed coat abrasion, and instrumental measurement inaccuracies during bench testing, the obtained performance metrics were marginally inferior to theoretical projections. Nevertheless, the empirical data demonstrate that the irregular slot-shaped seed metering device, engineered through optimal parameterization, fully complies with the technical standards for seeding apparatuses as stipulated in NY/T 1143—2006 (Technical Specifications for the Evaluation of Seeders)[32]. Specifically, it satisfies all critical performance criteria—seed germination rate, reseeding frequency, and seed loss ratio—thereby substantiating its operational efficacy in precision rapeseed sowing applications.

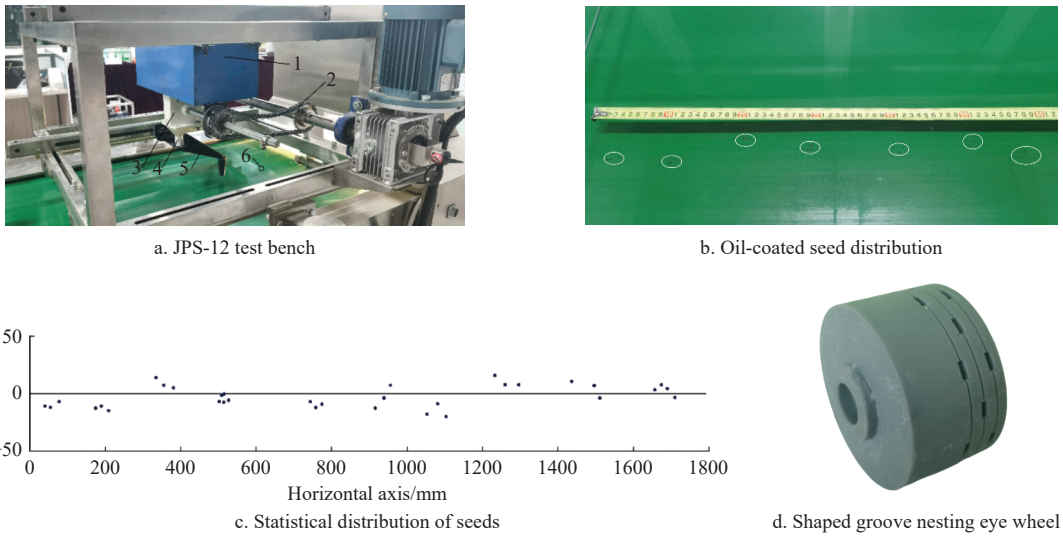

a. JPS-12 test bench

b. Oil-coated seed distribution

c. Statistical distribution of seeds

d. Shaped groove nesting eye wheel

1. Seed box 2. Drive chain 3. Seed dispenser 4. Funnel 5. Inoculation funnel 6. Seeds

Figure 14 Seed displacer bench test and seed distribution

Table 10 Test results of seed metering device on bench

Number	Number of grains/grain							Total number of grains in hole/grain	Qualified seeding rate/%	Reseeding rate/%	Missed seeding rate/%	Damage rate/%
	0	1	2	3	4	5	6					
1	0	2	26	59	32	7	2	128	91.41	7.03	1.56	1.56
2	4	7	23	63	33	3	0	133	89.47	2.26	8.27	0.75
3	2	8	31	72	39	5	1	158	89.87	3.8	6.33	1.27
4	1	3	28	66	36	6	4	144	90.28	6.94	2.78	0.69
5	2	2	23	55	28	6	2	118	89.83	6.78	3.39	0.85
Average	-	-	-	-	-	-	-	-	90.17	5.36	4.47	1.02

5 Field experiment

The Gansu region features a narrow and elongated topography, with rapeseed cultivation widely distributed across various subregions. According to existing studies[33], in the Hexi Corridor—including areas such as Jiuquan and Zhangye—rapeseed is predominantly sown using ridge-furrow row planting. In these areas, the typical row spacing ranges from 30 to 40 cm, while the ridge width, ridge surface width, and inter-ridge furrow width fall between 1.2-1.5 m, 0.8-1.0 m, and 0.4-0.5 m, respectively. In the arid Loess Plateau regions of central Gansu, including Lanzhou and Dingxi, full-film hole sowing and ridge-film furrow sowing are the most common practices. These methods generally employ a row spacing of 25-30 cm, ridge widths of 60-70 cm, and furrow widths of 30-40 cm. Hezheng County, located in Linxia Hui Autonomous Prefecture at the upper reaches of the Yellow River, follows similar agronomic standards to those of the central Loess Plateau. Here, ridge-furrow planting is also the predominant method, with typical row spacing of 25-30 cm and plant spacing of 12-15 cm.

To assess the adaptability of the precision seeder in practical agricultural contexts, this study referred to prior literature[34] and identified that the dominant soil types at the Hezheng experimental site comprise a mixture of yellow loam and gray calcareous soils. These soils possess a sandy texture that is friable and easily workable, making them well-suited for mechanical precision seeding. Prior to sowing, soil moisture in the 0-20 cm plow layer

was measured, revealing an average content of 15.45% and a bulk density of approximately 1.54 g/cm^3. This moderate moisture level provided favorable conditions for seed embedment and positional stability, thereby reducing seed displacement and minimizing coat damage.

The field experiment was conducted in Hezheng County, Gansu Province, in April 2024, using the 2BF-12 precision rapeseed seeder co-developed by Gansu Agricultural University and Dingxi Sanniu Co., Ltd. Sowing trials were performed under optimal parameter settings to evaluate the performance of the shaped groove eyelet wheel seed dispenser. The rapeseed cultivar used was "Longyou 19." The sowing operation was powered by a Dongfeng Hong MF704 tractor (Yituo Group, Luoyang, Henan, China) operating at a forward speed of 1.73 km/h. The machine could simultaneously sow six rows at a row spacing of 30 cm. The sowing process and resulting seedling emergence are illustrated in Figure 15. One month after planting, seedling emergence was assessed by randomly selecting six rows and counting the number of rapeseed plants within one meter of each row to calculate average performance metrics. Statistical analysis indicated that the qualified seedling rate [(3±1) plants per hole] reached 89.31%, the replanting rate [more than (3±1) plants per hole] was 4.17%, and the omission rate [fewer than (3±1) plants per hole] was 6.52%. The average number of rapeseed plants per hole was 3.22. The test results were evaluated with reference to NY/T 1143—2006, Technical Specifications for the Evaluation of Seed Drill Quality (Table 11), meeting the agronomic requirements for rapeseed cultivation in the region.

Figure 15 Field test and seedling emergence effect

Table 11 Test results of field experiment

Parameters	Research equipment	Technical specifications
Qualification rate of seeds per hole/%	89.31	≥85
Replay index/%	4.17	≤30
Missed broadcast index/%	6.52	≤15
Seed damage rate/%	0.82	≤1.5

6 Conclusions

Due to the simplistic structure and small size of the seed guide groove in traditional nesting wheels, this study was inspired by geometrical principles to design a nesting wheel featuring a shaped groove with a trapezoidal seed guide. This design aims to enhance seed filling efficacy. The fundamental dimensions of the shaped groove were established through structural analysis, followed by a force analysis of the seeds within the groove. It was determined that the primary factors influencing the seed filling performance of the seed discharge wheel included the inclination angle of the seed guide groove, the width of the trapezoidal seed guide groove, the width of the shaped groove, and the rotational speed of the seed discharge wheel. The basic ranges for each influencing factor were established through one-factor tests, and the response surface methodology was employed to optimize and identify the optimal combination of parameters. Ultimately, the results of bench and field tests conducted under the optimized conditions indicated that the designed shaped notch nesting wheel meets the agronomic standards for rapeseed cultivation in Gansu Province, China. The specific conclusions are as follows:

1) The design of the traditional wheel-type seed metering device with special-shaped holes was enhanced by converting the rectangular seed guide groove into a trapezoidal shape. Key dimensions of the shaped groove wheel were established as follows: a wheel diameter of 74 mm, a hole length of 6.60 mm, a hole width of 2.35 mm, and a hole height of 2.25 mm. The trapezoidal seed guide groove has a width of 5.50 mm and a depth of 1.50 mm. A total of 21 holes are arranged in three rows, with seven holes in each row.

2) Based on the force analysis during the seed-filling process, four key factors were identified as critical to seed metering performance: the inclination angle of the seed guide groove, the rotational speed of the shaped groove eyelet wheel, the width of the trapezoidal seed guide groove, and the width of the shaped groove. Using the EDEM simulation platform, both single-factor simulations and a second-order regression orthogonal rotational combination experiment were conducted to evaluate the relative significance of each parameter. The analysis revealed that, for the qualification rate of seeds per hole, the most influential factors were the wheel's rotational speed followed by the inclination angle of the guide groove. For the reseeding rate, the order of influence was: rotational speed, shaped groove width, guide groove angle, and trapezoidal groove width. In the case of missed seeding, the dominant factors were rotational speed, shaped groove width, and guide groove angle. Optimization of the regression model yielded the following ideal parameter combination: a seed guide groove inclination of 20°, a trapezoidal groove width of 6.5 mm, a shaped groove width of 2.21 mm, and a wheel rotation speed of 19.10 r/min. Under these conditions, the simulation predicted a seed qualification rate of 94.17%, a reseeding rate of 3.92%, and a missed seeding rate of 1.91%. Subsequent bench tests confirmed the simulation outcomes, delivering a qualified seeding rate of 90.17%, a reseeding rate of 5.36%, a missed seeding rate of 4.47%, and a seed damage rate of 1.02%. All results satisfied the agronomic requirements for precision rapeseed sowing.

3) Under the optimized parameter conditions, field tests were conducted using the shaped groove eyelet wheel seed metering device, with seedling emergence assessed post-sowing. The qualified rate of plants per hole (3±1 plants) reached 89.31%, and the average number of rapeseed plants per hole was 3.22, fulfilling the agronomic requirements for rapeseed planting.

Acknowledgements

The authors also acknowledge the financial support for this work provided by the National Natural Science Foundation of China (Grant No. 52065004 and Grant No. 52365030); Lanzhou Municipal Young Talent Innovation Project (Grant No. 2023-QN-146); Major Cultivation Project of Collegiate Scientific Research and Innovation Platform of Gansu Provincial Department of Education (Grant No. 2024CXPT-15); Special Project of Gansu Provincial Commissioner for Science and Technology (Grant No. 23CXGA0066); Gansu Agricultural Machinery R&D, Manufacturing and Promotion of Application in 2023 Integrated Pilot Project (3-3).

[References]

[1] Gao H R, Teng S L, Luo Y X. Preliminary analysis of transcriptomes of different Brassica napus petals. Journal of Northwest A & F University(Natural Science Edition), 2024; 52(9): 51–61.

[2] Jin X. Modern vegetable nursery and planting technology and equipment. Beijing: Machinery Industry Press. 2018; 265p. (in Chinese)

[3] Wu C Y, Wang J H, Yang Y, Li D Y, Li X, Yan R. Analysis of the development status and mechanization trends of economic crop industry in China. Journal of Chinese Agricultural Mechanization, 2024; 45(1): 1–13.

[4] Lin L B, Zhang C L, Xia G Y, Ma Z Q. Rapeseed is an advantageous energy crop for biodiesel development. In: Proceedings of 2006 Annual Academic Conference of the Crop Society of China, Harbin, China: Crop Society of China, 2006; 5. (in Chinese)

[5] Li X, Hu Q S, Wang X S, Gong M, Liu D W, Xie F P. Design and experiment of a single needle vibrating pneumatic pepper precision seed dispenser. Acta Agriculturae Universitatis Jiangxiensis, 2024; 46(4): 749–762.

[6] Yazgi A, Degirmencioglu A. Optimization of the seed spacing uniformity performance of a vacuum-type precision seeder using response surface methodology. Biosystems Engineering, 2007; 97(3): 347–356.

[7] Bilandžija N, Fabijanić G, Kiš D. Effect of precision drill forward speed on in-row seed spacing accuracy of red beet. Tehnički Vjesnik – Technical Gazette, 2017; 24(4): 963–966.

[8] Shi S, Zhang D X, Yang L, Cui T, Zhang R, Yin X W. Design and experiment of the pneumatic maize precision seed-metering device with combined holes. Transactions of the Chinese Society of Agricultural Engineering, 2014; 30(5): 10–18.

[9] Wu F T. Research on the positive and negative air pressure combination of rapeseed precision direct seeding rower. Master dissertation. Wuhan: Huazhong Agricultural University, 2007; 83p. (in Chinese)

[10] Yan Y Q, Liu L J, Liu Y Q, Wu H H, Lu Q, Liu F J. Design and test of four-stage seed cleaning mechanism for air-suction vegetables seed-metering device. Transactions of the Chinese Society for Agricultural Machinery, 2023; 54(S1): 57–65.

[11] Li P W, Tian B, Sun W, Zhang H, Liu X L, Li H. Current status and outlook of the development of potato precision seeding technology. Agricultural Equipment & Vehicle Engineering, 2024; 62(1): 29–33.

[12] Zhang X Q, Wang D M, Zhu S Q, Wang Z Y, Li H G. Development of the 2BYM-3 precision seeder for leafy industrial hemp. Transactions of the Chinese Society of Agricultural Engineering, 2023; 39(7): 97–104.

[13] Liu T, He R Y, Lu J, Zou L, Zhao M M. Simulation and verification on seeding performance of nest hole wheel seed-metering device based on EDEM. Journal of South China Agricultural University, 2016; 37(3): 126–132.

[14] Lai Q H, Jia G X, Su W, Hong F W, Zhao J W. Design and test of ginseng precision special-hole type seed-metering device with convex hull. Transactions of the Chinese Society for Agricultural Machinery, 2020; 51(7): 60–70.

[15] Bao Y H. Design and testing of a hole-wheel type seed dispenser for Isatis indigotica (Ban Lan Gen) hole sowing. Master dissertation. Daqing: Heilongjiang Bayi Agricultural University, 2021. 71p. (in Chinese)

[16] Peng F, Wang J Q, Zhang L, Wei C Y, Liu W L, Wang X Y, et al. Improvement and parameter optimization of the air-suction seed-metering device for *Cyperus esculentus* L. Agricultural Engineering, 2022; 12(12): 98–103. (in Chinese) doi: 10.19998/j.cnki.2095-1795.2022.12.017.

[17] Zhao Z F. Design and test of spoon-type Cyperus esculentus seeder. Master dissertation. Changchun: Jilin Agricultural University, 2022. 68p. (in Chinese)

[18] Liu C L, Wei D, Du X, Jiang M, Song J N, Zhang F Y. Design and test of wide seedling strip wheat precision hook-hole type seed-metering device. Transactions of the Chinese Society for Agricultural Machinery, 2019; 50(1): 75–84.

[19] Cao C M, Ding W Y, Liu Z B, An M H, Zhang X C, Qin K. Design and experiment of seed disperser for ning-guo radix peucedani based on rocky dem. Transactions of the Chinese Society for Agricultural Machinery, 2023; 54(8): 53–64. (in Chinese)

[20] Liao Y T, Liu J C, Liao Q X, Zheng J, Li T, Jiang S. Design and test of positive and negative pressure combination roller type precision seed-metering device for rapeseed. Transactions of the Chinese Society for Agricultural Machinery, 2024; 55(5): 63–76. (in Chinese)

[21] Gai M M, Yang J, Li X H, Qu Z, Li H, Yu Y C. Design and test of guided horizontal disc soybean precision seeder. Jiangsu Agricultural Sciences, 2023; 51(22): 200–206.

[22] Tai Q L. Design and experiment of adjustable socket-eye precision fertilizer feeder. Master dissertation. Hefei, Anhui: Anhui Agricultural University, 2020; 73p. (in Chinese)

[23] Lin H Y, Wang G H, Guo Z W, Yuan X, You Y. Design and experiment of special-shaped seed cell for alfalfa precision seed metering device. Journal of Agricultural Mechanization Research, 2023; 45(11): 82–90. (in Chinese)

[24] Ge H, He H B, Li H Y, Mao Y F, Shi Z G, Chen X Y. The design for the nest-eye wheel type soybean seed-metering device based on EDEM. Journal of Shandong Agricultural University (Natural Science Edition), 2023; 54(1): 150–158. (in Chinese)

[25] Sun L S. Design and experimental study of the flat fritillary belt eyelet seeding device. Master dissertation. Daqing, Heilongjiang: Heilongjiang Bayi Agricultural University, 2022; 91p. (in Chinese)

[26] Wang B S, Wang L, Liao Y T, Wu C, Cao M, Liao Q X. Design and test of seeding wheels of precision hole-seeding centralized metering device for small particle size seeds. Transactions of the Chinese Society for Agricultural Machinery, 2022; 53(11): 64–75, 119.

[27] Liu R R. Analysis of pore group effect and performance test of quinoa pneumatic precision seed metering. Master dissertation. Hohhot, Inner Mongolia: Inner Mongolia Agricultural University. 2023; 61p. (in Chinese)

[28] Li H, Yuan Q, Zhang X, Yang W C, Tang X Y, Chen S C. Mechanical model of precision seeding for Panax notoginseng seed-metering device with nest-eye wheel. Journal of Agricultural Mechanization Research, 2015; 37(9): 22–26. (in Chinese)

[29] Cao X L, Li Z H, Li H W, Wang X C, Ma X. Measurement and calibration of the parameters for discrete element method modeling of rapeseed. Processes, 2021; 9(4): 605.

[30] Rao G, Zhao W Y, Shi L R, Sun B G, Guo J H, Wang Z. Calibration and experimental validation of discrete element simulation parameters for double-low rapeseed. Journal of China Agricultural University, 2023; 28(11): 192–207. (in Chinese)

[31] Lai Q H, Cao X L, Yu Q X, Sun K, Qin W. Design and experiment of a precision seeding device for hole-drop planter for Panax notoginseng. Transactions of the Chinese Society for Agricultural Machinery, 2019; 50(1): 85–95. (in Chinese)

[32] NY/T 1143—2006. Technical specification for quality evaluation for drills. Industry Standard - Agriculture; 2006. (in Chinese)

[33] Wang T, Zheng G, Lü X D, Liu Z X. Developing high-efficiency fertilization models for spring rapeseed in Hexi Corridor of Gansu Province. China Agricultural Technology Extension, 2019; 35(S1): 138–140. (in Chinese)

[34] Zhou B. Research on integrated construction technique of standardized terrace in Gansu province. Master dissertation, Xi'an: Xi'an University of Technology. 2017; 131p. (in Chinese)